Lawrence Berkeley National Laboratory

Title
Control of the Magnetic and Magnetotransport Properties of La0.67Sr0.33MnO3 Thin Films Through Epitaxial Strain

Permalink
https://escholarship.org/uc/item/48v97189

Authors
Takamura, Y.
Chopdekar, R.V.
Arenholz, E.
et al.

Publication Date
2008-04-21

Control of the Magnetic and Magnetotransport Properties of $La_{0.67}Sr_{0.33}MnO_3$ Thin Films Through Epitaxial Strain

Y. Takamura[1,2], R.V. Chopdekar[2,3], E. Arenholz[4], and Y. Suzuki[2]

[1] Department of Chemical Engineering and Materials Science, University of California, Davis, Davis, CA

[2] Department of Materials Science and Engineering, University of California, Berkeley, CA, and Materials Science Division, Lawrence Berkeley National Laboratory, Berkeley, CA

[3] School of Applied Physics, Cornell University, Ithaca, NY

[4] Advanced Light Source, Lawrence Berkeley National Laboratory, Berkeley, CA

The influence of epitaxial strain, in the form of tetragonal distortions, on the magnetic and magnetotransport properties of $La_{0.67}Sr_{0.33}MnO_3$ thin films was studied. The tetragonal distortion (c/a ratio) was modulated through the choice of the substrate, ranging from c/a=1.007 on (001)-oriented $(LaAlO_3)_{0.3}(Sr_2AlTaO_6)_{0.7}$ substrates to 0.952 on (110)-oriented $GdScO_3$ substrates. In agreement with previous theoretical predictions, these large values of tensile strain cause the Curie temperature and the saturation magnetization to decrease, alter the temperature dependence of the resistivity and magnetoresistance, and increase the resistivity several orders of magnitude.

The Control of Magnetic Domain Patterns in $La_{0.67}Sr_{0.33}MnO_3$ Thin Films Through Epitaxial Strain

Highly spin polarized materials, such as the doped rare-earth manganites $R_{1-x}A_xMnO_3$, where

R=trivalent lanthanide and A=divalent alkaline earth, are attractive candidates for memory and

sensor applications due to the high degree of spin-polarization of the carriers at the Fermi level,

the observation of colossal magnetoresistance (CMR), and its Curie temperature, T_c, in excess of

room temperature. Furthermore, the magnetic and electronic properties depend strongly on

parameters such as lattice strain,[1-3] external hydrostatic pressure,[4,5] oxygen stoichiometry,[6] and

the doping level, x.[5,7] As an example, Konishi and coworkers[8,9] constructed a phase diagram of

the magnetic ground states showing that the transitions between ferromagnetic (FM) and

antiferromagnetic (AF) states can be controlled through the doping level and the tetragonal

distortion (c/a ratio) of the structure imposed from the substrate.   They predicted that due to the

coupling of the orbital ordering of the e_g states with the Jahn Teller distortions of the MnO_6

octahedra, the film transitions from the FM/metal state when unstrained to an AF/insulator state

(type C) at large compressive strains and to an AF/metal (type A) state under large tensile

strains.[8,9] Experimental results in the literature have shown decreased magnetization and

insulating behavior for $La_{0.7}Sr_{0.3}MnO_3$ films grown on $LaAlO_3$ (LAO) substrates[1,8] (lattice

mismatch ~2.16%, c/a=1.06) ascribed to the type C antiferromagnetic state, while the type A

state was observed in $La_{0.5}Sr_{0.5}MnO_3$ and $Nd_{0.55}Sr_{0.45}MnO_3$ samples.[8] In addition, it has been

shown that in LSMO thin films, moving from compressive strain on LAO substrates to tensile

strain on STO substrates changes the easy magnetization direction from out-of-plane to in-

plane.[10-13] In this work, we choose a fixed composition, $La_{0.67}Sr_{0.33}MnO_3$ (LSMO) and report for

the first time epitaxial strain extending from small compressive strain (c/a=1.007) to large tensile

strain (c/a=0.952). These samples permit the experimental verification of Konishi's model

The Control of Magnetic Domain Patterns in La$_{0.67}$Sr$_{0.33}$MnO$_3$ Thin Films Through Epitaxial Strain

concerning the effect of these large values of tensile strain on the magnetic and magnetotransport properties of LSMO thin films.

The epitaxial strain of the LSMO thin films is varied through the choice of the substrate type, including (001)-oriented (LaAlO$_3$)$_{0.3}$(Sr$_2$AlTaO$_6$)$_{0.7}$ (LSAT, a=3.87 Å) and SrTiO$_3$ (STO, a=3.905 Å) as well as (110)-oriented DyScO$_3$ (DSO, a=5.44 Å, b=5.71 Å, and c=7.887 Å) and GdScO$_3$ (GSO, a=5.488 Å, b=5.746 Å, and c=7.934 Å). Bulk LSMO has a rhombohedral crystal structure with a pseudocubic lattice parameter a~3.88 Å and the resulting lattice mismatch ranges from -0.26% when grown on LSAT substrates to +2.44/2.59 % on GSO substrates relative to the substrate $\left[\bar{1}\,10\right]$ and $\left[001\right]$ directions, respectively.

The LSMO films were grown by pulsed laser deposition. The KrF laser (248 nm) was operated between 1 and 3 Hz with a fluence ~1.2 J/cm^2, while the substrate temperature was held at 700°C and the oxygen pressure was 320 mTorr. The samples were cooled slowly to room temperature in an oxygen pressure of ~300 Torr to assure the proper oxygenation of the films. Surface morphology was investigated by atomic force microscopy (AFM) while the structural properties of the films were measured by high-resolution x-ray diffraction (XRD) using a Bruker D8 Discover four-circle diffraction system. Magnetotransport properties of the films as a function of temperature were measured using the van der Pauw geometry with the magnetic field applied in the plane of the film. X-ray absorption spectra (XAS) and x-ray magnetic circular dichroism (XMCD) experiments were performed at beamlines 4.0.2 and 6.3.1 of the Advanced Light Source.[14] With these techniques, the surface sensitivity is determined by the electron escape depth (~5-10 nm) and the spectra were recorded using total electron yield by monitoring the

The Control of Magnetic Domain Patterns in $La_{0.67}Sr_{0.33}MnO_3$ Thin Films Through Epitaxial Strain

sample drain current as function of x-ray energy. For the XMCD measurements, the x-ray incidence angle was 30° to the surface with the applied field parallel to the x-rays. The XMCD difference spectra were obtained with fixed x-ray polarization and opposite applied fields of 0.27 T.

The surface morphology of the LSMO grown on the various substrates was measured using AFM. All films are extremely smooth with rms roughness values below 0.5 nm, irrespective of the epitaxial strain imposed by the substrate. XRD θ-2θ scans of the out-of-plane direction and reciprocal lattice maps of the (103) LSMO reflection reveal that regardless of substrate type, the LSMO films are fully strained to the substrate which results in tetragonal distortions ranging from 1.007 on LSAT substrates down to 0.952 on GSO substrates as described in Table 1. For the LSMO/GSO films a slight asymmetry and a decreased intensity of the film peak relative to the films grown on other substrates suggest a reduced epitaxial film quality and a distribution of lattice parameters throughout the film thickness. This value of tetragonal distortion approaches the value predicted by Konishi *et al.*[8,9] for the transition between the FM/metallic state to the AF/metal state (type A). These results demonstrate that the strain of the LSMO film can effectively be tuned by the choice of substrate, however, a lower limit may exist on the value of tetragonal distortion (c/a~0.96) that can be achieved in LSMO thin films.

The XA spectra around the Mn L_3 absorption edge for LSMO films on the various substrates are plotted in Figure 1(a). The LSMO films under large tensile strain on the DSO and GSO substrates display an extra feature on the low energy side of the main peak not found in the LSMO/STO film. Tentatively, this feature has been ascribed to an increased concentration of

Mn^{3+} by comparison with representative spectra in the literature.[15,16] This increase in Mn^{3+} concentration could arise due to a change in the La:Sr ratio near the surface or substrate interface mediated by the large tensile strain.

Because of the large paramagnetic contribution from the scandate substrates, bulk magnetometry measurements could not be performed. Instead we performed XMCD measurements to probe the surface magnetic properties of the LSMO films. Figure 1(b) and (c) plot the Mn XMCD difference spectra for the 35 nm thick LSMO films grown on the various substrates. At room temperature, the LSMO/LSAT film is ferromagnetic, while no appreciable ferromagnetic order is observed for the LSMO films under large tensile strain on DSO and GSO substrates. At 30 K, the LSMO/LSAT film displays a large XMCD signal while bulk magnetometry shows that the film possesses the expected saturation magnetization of 3.6 μ_B/Mn. At this low temperature, the LSMO/DSO and LSMO/GSO films both become magnetic, though the saturation magnetization is depressed by 10% and 40%, respectively, compared to the value observed for the LSMO/LSAT film. Interestingly, the LSMO/DSO film displays the smallest average moment despite the fact that the LSMO/GSO film possesses the largest tetragonal distortion. Instead of the characteristic sharp magnetic transitions with a coercive field less than 100 Oe, the hysteresis loops of the LSMO films on GSO and DSO (not shown) are characterized by the gradual rotation of the moments into the direction of the applied magnetic field with a significant increase in the coercive field to ~900 Oe and 1200 Oe, respectively. These results indicate that the magnetic properties of the films are dramatically altered by large values of tensile strain ($c/a<0.962$) with a decrease in T_c to temperatures below room temperature.

The Control of Magnetic Domain Patterns in $La_{0.67}Sr_{0.33}MnO_3$ Thin Films Through Epitaxial Strain

The CMR oxides such as LSMO are characterized by coincident metal/insulator (MIT) and

FM/paramagnetic transitions that occur at the Curie temperature, T_c~360 K for bulk material.

The magnetoresistance, $MR = [\rho(H = 5T) - \rho(H = 0T)]/\rho(H = 0T)$ shows a peak at the same

temperature, as the applied magnetic field has the greatest effect on ordering the Mn spins at the

temperature with the greatest disorder. Figure 2 plots resistivity and MR as a function of

temperature for 35 nm thick LSMO films grown on the various substrates. The LSMO films

grown under a small tensile (STO) or compressive (LSAT) strain show the expected shape for

the resistivity curve with a MIT and a peak in MR which occurs at T_c~340 K, slightly reduced

from the bulk value. In contrast, the resistivity of the LSMO films grown with large tensile

strain on GSO and DSO substrates increases by several orders of magnitude compared to the

films grown on STO or LSAT substrates. The shape of the resistivity curves is changed

substantially, showing weak temperature dependence at lower temperatures. A broad

metal/insulator transition occurs near 200 K with a weaker feature near 100 K. In concert, the

MR curves reach a plateau around –45% below 200 K. Despite having the lower tetragonal

distortion, the LSMO/DSO film has a larger resistivity over the entire temperature range studied

compared to the LSMO/GSO film. These results corroborate the XMCD measurements,

indicating a significant change in the magnetic and magnetotransport properties of LSMO with

large values of tensile strain.

Table 1 summarizes the magnetic and magnetotransport properties for the LSMO thin films

grown on the various substrates with c/a ranging from 1.007 to 0.952. For comparison, the

corresponding information for an LSMO/LAO film with c/a=1.06 from the work of Konishi et

al.[8] has been included. In agreement with the first principles calculations[9] and previous

experimental results[8], the LSMO films grown under small tensile or compressive strain are FM/metals with a $T_c{\sim}340$ K. As c/a decreases below ~0.960, a transition to the Type A, AF/metal state was predicted. [9] Our experimental results for LSMO/DSO films (c/a=0.962) demonstrate a broad MIT at ~200 K and weak ferromagnetism which may be interpreted as the onset of the AF state.   In addition, we observe that T_c drops below room temperature and the resistivity increases by several orders of magnitude, compared to the value for LSMO/STO and LSMO/LSAT films. Despite the smaller c/a ratio, the LSMO/GSO film displays a larger average moment and lower resistivity compared to the LSMO/DSO film. However, one must consider the reduced epitaxial quality of the LSMO/GSO film and the distribution of lattice parameters throughout the film thickness. It is likely that the relaxed portion of the film consists of the FM/metal phase and that it resides at the surface of the film which is probed by the XMCD measurements.   Therefore, these results confirm that both compressive and tensile strain can be used to control the magnetic phase in LSMO films, however, a lower limit may exist on the value of tetragonal distortion ($c/a{\sim}0.96$) that can be achieved.

In conclusion, we have investigated the effect of epitaxial tensile strain on the magnetic and magnetotransport properties of LSMO thin film. The tetragonal distortion can effectively be tuned between 1.007 and 0.952 by varying the substrate type. Increasing the magnitude of tensile strain decreases the T_c and the saturation magnetization, changes the temperature dependence of the resistivity and the magnetoresistance, and increases the resistivity of the LSMO film by several orders of magnitude. These strain induced changes may be related to a change in the La:Sr ratio at the film surface or interface with the substrate and/or the coupling of the orbital ordering of the e_g state with the Jahn-Teller distortions of the MnO_6 octahedra.

The Control of Magnetic Domain Patterns in La$_{0.67}$Sr$_{0.33}$MnO$_3$ Thin Films Through Epitaxial Strain
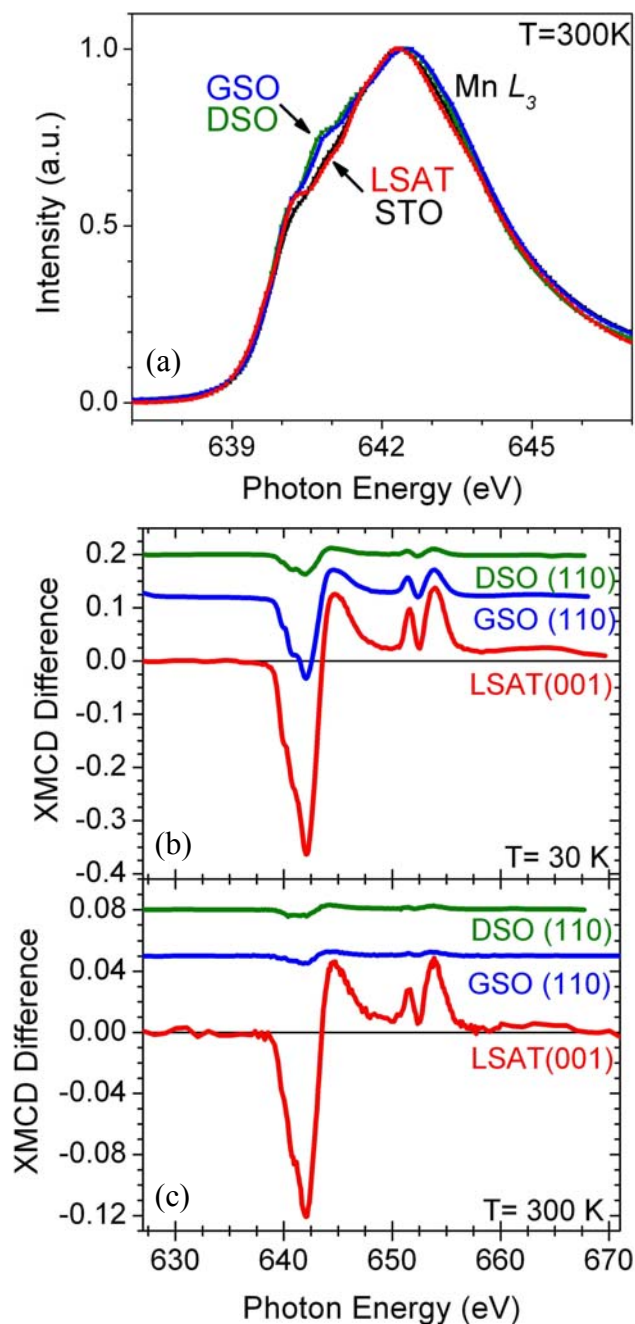
Figure 1: (a) XA spectra of the Mn L_3 edge and XMCD difference spectra measured at (b) 30 K and (c) 300 K for a 35 nm thick LSMO films on LSAT, GSO, and DSO substrates.
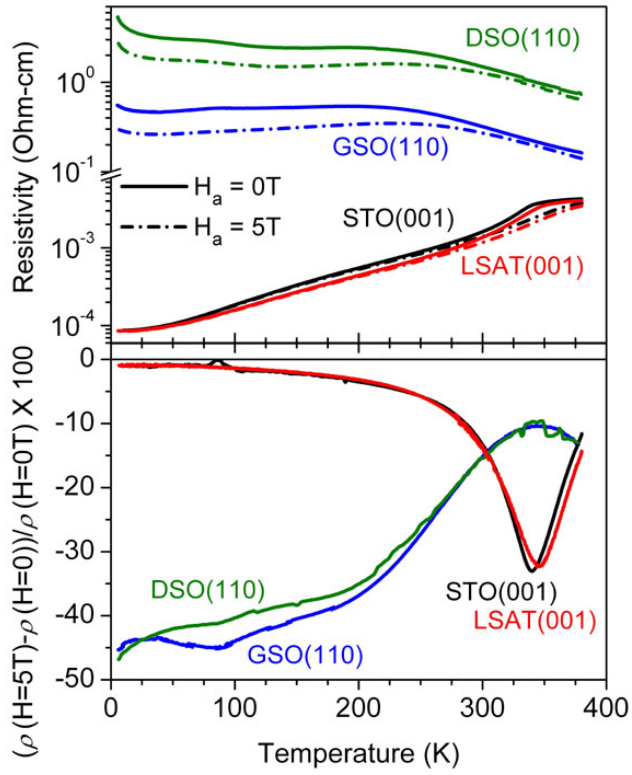
Figure 2: (a) Resistivity and (b) *MR* as a function of temperature for 35 nm thick LSMO films on LSAT, STO, GSO, and DSO substrates.

Table I. Summary of the LSMO films grown on various single crystal oxide substrates

Substrate	$t_{(LSMO)}$ (nm)	$a_\perp$ (Å)	c/a	Theory[9]	XMCD	Resistivity/*MR*
LAO[8]	40	4.2	1.06	AF insulator	--	Insulating
LSAT	40	3.896	1.007	FM metal	FM at 300 K	MIT at 340 K
STO	35	3.842	0.984	FM metal	FM at 300 K	MIT at 340 K
DSO	35	3.796	0.962	AF metal	Small average moment at 30 K	~MIT at 200 K
GSO	35	3.785	0.952	AF metal	FM at 30 K	~MIT at 200 K

[1]   F. Tsui, M. C. Smoak, T. K. Nath, and C. B. Eom, Appl. Phys. Lett. **76,** 2421-2423 (2000).

[2]   Y. Suzuki, H. Y. Hwang, S.-W. Cheong, and R. B. van Dover, Appl. Phys. Lett. **71,** 140-142 (1997).

[3]   S. Jin, T. H. Tiefel, M. McCormack, H. M. O'Bryan, L. H. Chen, R. Ramesh, and D. Schurig, Appl. Phys. Lett. **67,** 557-559 (1995).

[4]   H. Y. Hwang, T. T. M. Palstra, S.-W. Cheong, and B. Batlogg, Phys. Rev. B **52,** 15046-15049 (1995).

[5]   Y. Moritomo, A. Asamitsu, and Y. Tokura, Phys. Rev. B **51,** 16491-16494 (1995).

[6]   J. F. Mitchell, D. N. Argyriou, C. D. Potter, D. G. Hinks, J. D. Jorgensen, and S. D. Bader, Phys. Rev. B **54,** 6172-6183 (1996).

[7]   A. Urushibara, Y. Moritomo, T. Arima, A. Asamitsu, G. Kido, and Y. Tokura, Phys. Rev. B **51,** 14103-14109 (1995).

[8]   Y. Konishi, Z. Fang, M. Izumi, T. Manako, M. Kasai, H. Kuwahara, M. Kawasaki, K. Terakura, and Y. Tokura, J. Phys. Soc. Jpn. **68,** 3790-3793 (1999).

[9]   Z. Fang, I. V. Solovyev, and K. Terakura, Phys. Rev. Lett. **84,** 3169-3172 (2000).

[10]   C. Kwon, M. C. Robson, K. C. Kim, J. Y. Gu, S. E. Lofland, S. M. Bhagat, Z. Trajanovic, M. Rajeswari, T. Venkatesan, A. R. Kratz, R. D. Gomez, and R. Ramesh, J. Magn. Magn. Mater. **172,** 229-236 (1997).

[11]   A. M. Haghiri-Gosnet, J. Wolfman, B. Mercey, C. Simon, P. Lecoeur, M. Korzenski, M. Hervieu, R. Desfeux, and G. Baldinozzi, J. Appl. Phys. **88,** 4257-4264 (2000).

[12]   J. Dho, Y. N. Kim, Y. S. Hwang, J. C. Kim, and N. H. Hur, Appl. Phys. Lett. **82,** 1434-1436 (2003).

[13]   Y. Wu, Y. Suzuki, U. Rudiger, J. Yu, A. D. Kent, T. K. Nath, and C. B. Eom, Appl. Phys. Lett. **75,** 2295-2297 (1999).

[14]   E. Arenholz and S. O. Prestemon, Rev. Sci. Instrum. **76,** 183908 (2005).

[15]   M. Abbate, F. M. F. de Groot, J. C. Fuggle, A. Fujimori, O. Strebel, F. Lopez, M. Domke, G. Kaindl, G. A. Sawatzky, M. Takano, Y. Takeda, H. Eisaki, and S. Uchida, Phys. Rev. B **46,** 4511-4519 (1992).

[16]   F. M. F. de Groot, J. Electron Spectroscopy and Related Phenomena **67,** 529-622 (1994).